Condensation and Condenser Design
ASME 1993

PARTIAL CONDENSATION FROM STEAM-AIR MIXTURES IN HORIZONTAL TUBE HEAT EXCHANGERS

I. Lanzl, F. Mayinger, and G. Nolte
Technical University of München
München, Germany

ABSTRACT

Experimental investigations are reported for partial condensation of steam on a single horizontal tube and on a horizontal tube row with parallel flow. Local measurements of heat- and mass transfer were made in laminar and turbulent flow of the steam-air mixture in the two heat exchangers. Data have been obtained at near atmospheric pressure, with Reynolds numbers between $4.000 < Re < 17.000$ and a partial vapour pressure between $0.45 < p_{steam}/p_{total} < 0.95$.

The distribution of heat and mass transfer on a single horizontal tube is a function of the increasing air-fraction and the decreasing mass transport along the tube. In a tube row the heat- and mass transfer on the cooling tubes is additionally influenced by condensate inundation. The convective mass transport and the condensation of steam at the surface of the liquid film and at the condensate between the tubes cause a gradient of steam concentration and temperature in all three directions of the flow channel.

A dew-point probe with small size, specially developed for this investigations, was used to measure the local vapour concentration of the mixture in the heat-exchanger. The radial heat flux at the cooling tubes was measured by using the radial temperature gradient in the tubes.

The experiments in the single tube heat exchanger show near the inlet region a higher heat flux at the bottom of the tube than on the top although it should be smaller there due to a thicker liquid film. With increasing distance from the inlet the situation changes and the heat flux density gets its highest values at the top of the tube. The reason for the above mentioned effects is discussed for a better understanding of the condensation in vapour-gas mixtures. With the measured data correlations are developed for predicting the local Nusselt and Sherwood numbers in a horizontal annular-flow-channel. Preliminary values of measured heat flux densities in tube row heat exchanger are reported.

Introduction

Shell-side condensation is relevant to many important applications both in power engineering and in processing industry. Many experimental and theoretical investigations have been done in this field. A review is given by Marto [1].

A special point of interest in condensation experiments is the influence of non-condensable gases on the heat and mass transfer rates. Already small amounts of inert gas in vapour can cause a gradient of the air-fraction close to the condensate and may reduce significantly the condensation heat transfer rates. Differently from pure steam condensation, during partial condensation the steam is transferred by convection and diffusion. A temperature and concentration profile develops in the gas phase. Summaries of this phenomena are given by Chisholm [2] and Webb and Wanniarachchi [3]. In partial condensation the heat transfer coefficients, the gas compositions and the flow pattern vary along the path of mixture flow. Colburn and Hougen [4] developed a method to calculate shell-side heat transfer step by step along the path of mixture flow during partial condensation. Together with experimentally verified coefficients equations, partial condensation can be described with filmtheory. One of the recent publications on this field is given by Numrich and Rennhack [5]. Nolte [6] did experimental investigations on a single horizontal tube and developed coefficients equations for calculating heat- and mass transfer during partial condensation with the filmtheory. Several investigations are done in horizontal tube bundle heat exchangers, for example from Cavallini et al. [7]. All the known publications deal with a mixture flow perpendicular to the tube row.

The work reported here investigates the mechanism of heat- and mass transfer along a single horizontal tube and a horizontal tube row heat exchanger in parallel flow during the condensation of steam from a steam-air mixture. The heat- and mass transfer is mainly influenced by the condensing liquid film flowing around the cooled tubes and by the gradient of the air-fraction perpendicular to the tubes. Outside of the boundary layer the vapour concentration is constant in the bulk flow. The liquid leaving a tube and falling on the tube under it disturbs the boundary layer and the liquid film on both tubes. The increased turbulence in the liquid film and the boundary layer due to condensate inundation causes an increase in heat- and mass transfer. This effect is opposed by the decrease of heat- and mass transfer due to the higher film thickness on the inundated tubes.

Apparatus and Procedure

The investigation of condensation in the presence of an inert gas was performed in a test loop with the following main equipment as shown in Fig. 1: Steam is generated from destilled water in a boiler by three 15 kW-heaters. Compressed air is filtered from oil and dust. The steam- and air-flow rates are measured separately by a V-Cone probe and orifice flow meters. The air is passing an electrical heater before being mixed with the steam and enters then the heat exchanger. To avoid condensation on the way to the heat exchanger the steam is superheated according its higher pressure in the boiler.

For the single tube investigations, the heat exchanger is built up by two concentric tubes. The inner tube is cooled with water, the outer tube is isolated. The condensing gas mixture flows in the annulus between the outer and inner tube (hydraulic diameter $d_h = D_A - D_{II} = 15.5 \cdot 10^{-3} m$). To enable local measurements of heat and mass transfer along the heat exchanger tube with a condensing length of 2m a instrumented section with a length of 0.25m was installed and the gas

inlet was constructed movable in axial direction. This was achieved by a pipe consisting of two concentric tubes which were stuck movable into the gas annulus.
For the tube bundle investigations the heat exchanger is built up by three horizontal cooling tubes in a vertical row, one gas inlet, one gas outlet and one instrumented segment with a length of 0.25 m. Eight shell segments with different length can be fixed between the instrumented segment and the gas inlet. In both heat-exchangers the distance between the onset of condensation and the inlet of the instrumented segment can be varied from 0 to 1.75m in 0.25m steps in order to get eight measuring intervals at a total length of 2m.
Through the entire test loop, the steam-air mixture and condensate contacts only stainless steel, glass and Teflon seals. The loop was cleaned carefully to avoid contamination.

Instrumented segment

For the investigations in the heat exchangers the local heat and mass transfer along the tubes and the heat and mass transfer between the cooling surfaces of the tube row has to be calculated. Therefor local values of vapour concentration and temperature of the mixture, wall temperature of the cooling tubes and condensate mass flow at the bottom of the heat exchanger shells are measured. To obtain the local data of temperature and vapour concentration in the single tube heat exchanger the probes are mounted in a turning ring (Fig. 2). In the tube row, the probes are fixed in a rotatable disc (Fig. 3). In both arrangements the dew-point probe can be moved perpendicular to the tubes. With the rotating elements, together with the heat exchanger which allow variable condensation length before the instrumented segments, the local data can be obtained by one probe in each case.
The wall heat flux through the water cooled stainless steel tubes ($\emptyset 0.025m \times 0.005m$) is calculated from the wall temperatures of the tubes. Therefor the temperature gradient in the wall is used. In every tube four thermocouples ($0.5 \cdot 10^{-3}$ in diameter) were mounted - two flush mounted with the outer and two flush mounted with the inner surface. In order to get the circumferential temperature distribution the tubes can be turned.

Dew point probe

For measuring the vapour concentration a newly developed dew-point probe is used. The method is based on the determination of the dew-point temperature and the total pressure of the gas mixture. The design of the dew-point probe is shown in Fig. 4 and Fig. 5. The measuring sensor of the dew-point probe consists of a thermocouple soldered to a stainless steel foil, which is about 0.1mm thick, and separates the steam atmosphere from the channel system (Fig. 4). The stainless steel foil can be cooled from its rear side by a cooling gas. To do this, the capillary tubes of the channel system are connected to a cooling gas supply.
Without cooling the thermo-couple at the foil shows the true temperature of the steam-air mixture. As soon as the cooling is started, the temperature at the foil falls. Fig. 6 shows typical temperature curves. Curve a) was detected in pure air flow, curve b) was detected in a mixture of steam and air. Curve b) shows after the start of the cooling at first a decrease in the temperature until condensation begins at the outside of the foil. At this moment a sudden strong change in the temperature-time curve can be observed. This marks the dew-point temperature from which the steam concentrations in the mixture can be calculated. The next measurement can be started, after the condensate at the foil is evaporated. As the total pressure p does not exceed $\sim$ 10 bar and the presence of the non-condensing gas has negligible influence on the saturation

partial pressure, the air-concentration ($\dot{m}_a/\dot{m}_v$) can be calculated with the equations (1) and (2) and the measured saturation temperature T_s.

$$ln(p_s/mbar) = 19.0160 - \frac{4064.95}{(T_s/^oC) + 236.25} \tag{1}$$

$$\frac{m_a}{m_v} = \frac{p - p_s}{p_S} \times \frac{R_v}{R_a} \tag{2}$$

Experimental Results and Discussion

For the single tube heat exchanger experimental results are reported for the following inlet-conditions:

$T_{inlet} = 373K$ $\quad 4.370 < Re_{inlet} < 12.800 \quad 0.59 < p_{steam}/p_{total} < 0.95$.

The Reynols number is calculated as

$$Re = \frac{w_{mixture} \cdot (D_A - D_{II})}{\nu_{mixture}}$$

For the tube row preliminary results are reported for the following inlet-conditions:

$T_{inlet} = 373K$ $\quad 8.000 < Re_{inlet} < 17.000 \quad 0.45 < p_{steam}/p_{total} < 0.85$.

The Reynols number in this channel is calculated as

$$Re = \frac{(4 \cdot w_{mixture} \cdot A)}{\nu_{mixture} \cdot P_{wetted}}$$

Single tube heat exchanger

The varying heat- and mass transfer in the axial direction is mainly influenced by the decreasing steam flow rate and the increasing air-fraction in the boundary layer. The heat transfer from the gas to the wall is controlled by the heat flux due to the phase change of the condensing steam, the heat transport due to the convection in the gas annulus and the convective heat transport in the liquid film.

Due to the condensation of steam, the flow rate of the mixture and by this the velocity is decreasing along the tube. The velocity gradient along the tube is a function of the steam-air fraction and the Reynolds number at the gas inlet. Fig. 7 shows measured velocity gradients as a function of the inlet conditions.

Around the perimeter of the horizontal tube exists a gradient in air-concentrations, temperature and heat flux density. Thereasons for this effects are the increasing film thickness and the condensate dropping from the tube or being driven along the bottom of the tube by the air-steam flow. Fig. 8 shows an example of temperature and concentration profiles after a condensation length of 0.875 m and with the inlet conditions Re = 7.800 and $p_{steam}/p_{total} = 0.95$. Fig 8a) shows the temperature profiles at the film surface (t_f) and at the outer (t_{II}) and inner (t_I) tube wall. Fig 8b) shows the vapour concentration in the bulk flow (ψ_{vb}) and at the film surface (ψ_{vf}).

In a parallel flow heat exchanger the distribution of heat and mass transfer around the cooled surface varies along the tube. Fig. 9 shows the gradient of the heat flux density at four different positions at the tube perimeter. The data for $\varphi = 45^o$ and $\varphi = 105^o$ are similar, due to the laminar condensate film and the small increase of film thickness in this area. At the lower positions $\varphi = 180^o$ it can be observed, that the heat flux decreases with increasing film thickness. At higher vapour concentrations at the mixture inlet the heat flux at the tube bottom can be 30% smaller than the heat flux averaged over the perimeter.

Along the tube, the heat flux at the position $\varphi = 150^o$ can be 20% higher than the average value. The following effect is the reason for the increased heat flux in this position: A part of the condensate collects at the bottom of the tube and is driven along the surface by the shear stress from the mixture flow. This condensate forms drops, which flow along the tube, grow there and drop down after a while. The turbulence in the condensate film is enlarged by this drop motion. At a position $\varphi = 150^o$ the film is thin enough that the film turbulence cause an increase in heat flux. The condensate accumulation at the bottom of the tube builds up an heat transfer resistance, which can not be compensated by this turbulent motion.

From the measured values of heat flux, temperature differences and vapour concentrations, The Nusselt- and the Sherwood -numbers can be calculated. Comparing the results with the predictions of the film theory [8] shows interesting differences. In Fig. 10 the correction factor B

$$B = \frac{Sh(1-\psi_{vf})}{Sh_0} = \frac{\beta(1-\psi_{vf})}{\beta_0}$$

calculated by measured data and with the assumptions of the film theory is plotted versus the length of the channel. At the inlet, the experiment shows a higher correction factor than the theory predicts. This is due to inlet effects which are not described by the film theory. The upper picture shows correction terms for a fluid with a low vapour concentration at the mixture inlet. The Reynolds number along the tube is never smaller then 3.000. For this case, the film theory predicts at first rising and than falling correction terms. The experiment shows the opposite behaviour, at first a falling and then an increasing correction factor. Except for the inlet and outlet region the experimentally derived correction term is always smaller then the correction term predicted by the film theory. This effect can be explained by the theory for sucking of boundary layers derived by Schlichting [9]. The mass flow rate of the vapour towards the cooled surface on the tube can be regarded as such an effect, because during condensation the vapour is like a sucking off from the boundary layer. Therefor the turbulence in the boundary layer and by this the Nusselt- and Sherwood-number is reduced. In the lower picture the correction terms for a mixture with an higher amount of vapour at the inlet, and by this with lower Reynolds numbers along the tube are reported. The experimental data are higher then the predicted values. This is explained with the turbulence produced by the drops separating from the tube.

<u>Tube row heat exchanger</u>

The heat- and mass transfer during condensation in a tube row heat exchanger is a function of the thermodynamic and fluiddynamic effects described above for the single tube heat exchanger and, is additionally influenced by condensate inundation.

Fig. 11 and Fig. 12 show preliminary results obtained in the tube row. Fig. 11 shows the heat flux density, averaged over the perimeter, at the three horizontal cooling tubes after a condensation length of 2 m. The vapour concentration at the mixture inlet is $\dot{m}_a/\dot{m}_v = 0.55$, the Reynolds number at the inlet varies between 8.000 and 17.000. Fig. 12 shows the heat flux density at the some place, the Reynolds number at the inlet is constant $Re = 12.000$ and the inlet vapour concentration is increased from $\dot{m}_a/\dot{m}_v = 0.45$ to $\dot{m}_a/\dot{m}_v = 0.85$. The dominating transport resistance at partial condensation is built up by the vapour reduced boundary layer. On the inundated tubes the phase interface is moved by the surface waves in the condensate film. Additionally the boundary layer is disturbed by the condensate arriving at and leaving from the tubes. Both effects give rise to an increased turbulent exchange at an inundated tube in comparison to a single horizontal tube. Beside the boundary structure, temperature and vapour concentration in the bulk flow influences the distribution of heat flux densities at the tubes. The condensate at the cooling surfaces is subcooled relatively to the saturation temperature in the bulk flow. The thermal instability between the condensate leaving the tubes and the bulk flow, condensation occurs at the free condensate. The vapour concentration in the flow decreases and entails a decreased heat flux density. These effects lead to the intersection of the curves showing heat flux densities along the three cooling tubes.

Conclusion

The heat- and mass transfer during condensation out of an air-steam mixture was investigated in a single horizontal tube heat exchanger. The results were compared with the theoretical assumptions of the film theory. New correction terms were evaluated which allow to calculate partial condensation on a single horizontal tube in parallel flow by using the film theory.
Preliminary values are reported for a horizontal tube row heat exchanger. The work for the future will be to continue the experimental investigations in the tube row and develop a correlation for calculation heat- and mass transfer during partial condensation in a horizontal parallel flow tube row heat exchanger.

Acknowledgements

The authors wish to thank the Deutsche Forschungsgemeinschaft (DFG) for the financial support of this study.

[1] P.J. MARTO, "Heat Transfer and Two-Phase Flow during Shell-side Condensation", *Heat Transfer Engineering, vol.5, nos. 1-2,* (1984).

[2] D. CHISHOLM, " Modern Developments in Marine Condensers: Non condensable gases": An Overview in *Power Condenser Heat Transfer Technology*, eds. P. J. Marto and R. H. Nunn, pp 95-142, Hemisphere, New York, (1981).

[3] R.L. WEBB and A.S. WANIARACHCHI, " The Effects of Non condensable Gases in Water Chiller Condenser -Literature Survey and Theoretical Predictions, *ASHRAE Trans., vol. 86, pt. 1, pp. 142-159,* (1980).

[4] A.P. COLBURN and O.A. HOUGEN, " Design of Cooler Condensers for Mixtures of Vapours with Non condensing Gases", *Ind. Eng. Chem., vol. 26, pp.1178-1182,* (1934).

[5] R. NUMRICH and R. RENNHACK, " Heat and mass transfer during condensation of steam in the presence of air at pressures of up to 21 bar", ", *Chem. Eng. Technol. ,Vol. 12, pp. 235 - 244*, (1989).

[6] G. NOLTE, "Kondensation aus Dampf-Luft Gemischen im horizontal durchströmten Ringkanal", *Dissertation TU München*, (1989).

[7] A. CAVALLINI, S. FRIZZERIN, L. ROSETTO, "Condensation of R-11 vapour flowing downward outside a horizontal tube bundle", *Proc. of the Eighths Int. Heat Transfer Conference San Francisco,* CA U.S.A, (1986).

[8] BIRD, STEWART, LIGHTFOOD, " Transport Phenomena ", *John Wiley & Sons*, (1960).

[9] H. SCHLICHTING., "Grenzschicht Theorie", Verlag G. Braun, Karlsruhe, 5. Auflage, (1965)

Used symbols

A	$[m^2]$	area		**indices**
D	$[m]$	diameter	A	outer annulus diameter
$\dot{m}$	$[\frac{kg}{s}]$	air mass flow	a	air
p	$[\frac{N}{m^2}]$	pressure	b	bulk
P	[m]	perimeter	f	film surface
q	$[\frac{w}{m^2}]$	heat flux	s	saturation
R	$[\frac{J}{kgK}]$	Gas constant	v	vapour
T	$[K]$	Temperature	w	wall
w	$[\frac{m}{s^2}]$	velocity	I	inner cooling tube
ν	$[\frac{m^2}{s}]$	kinematic viscosity	II	outer cooling tube
ψ	[–]	pressure ratio $[\frac{p_v}{p_{total}}]$	0	with negligible mass transfer
			i	inlet

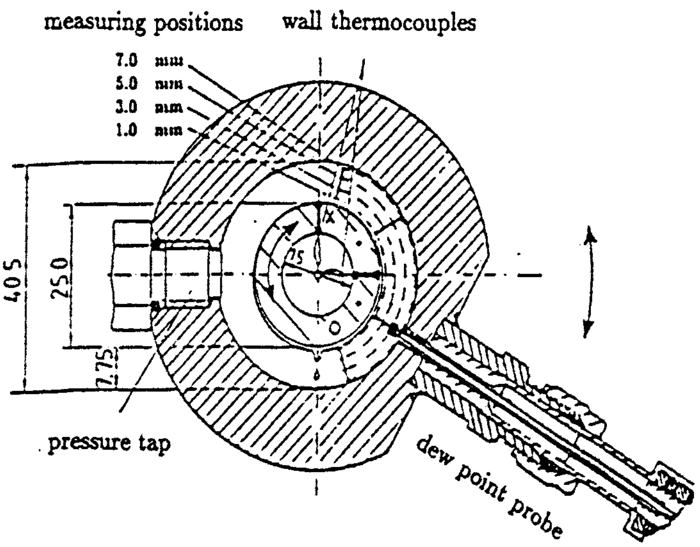

Fig. 2: Cross section of the instrumented segment in the single tube heat exchanger

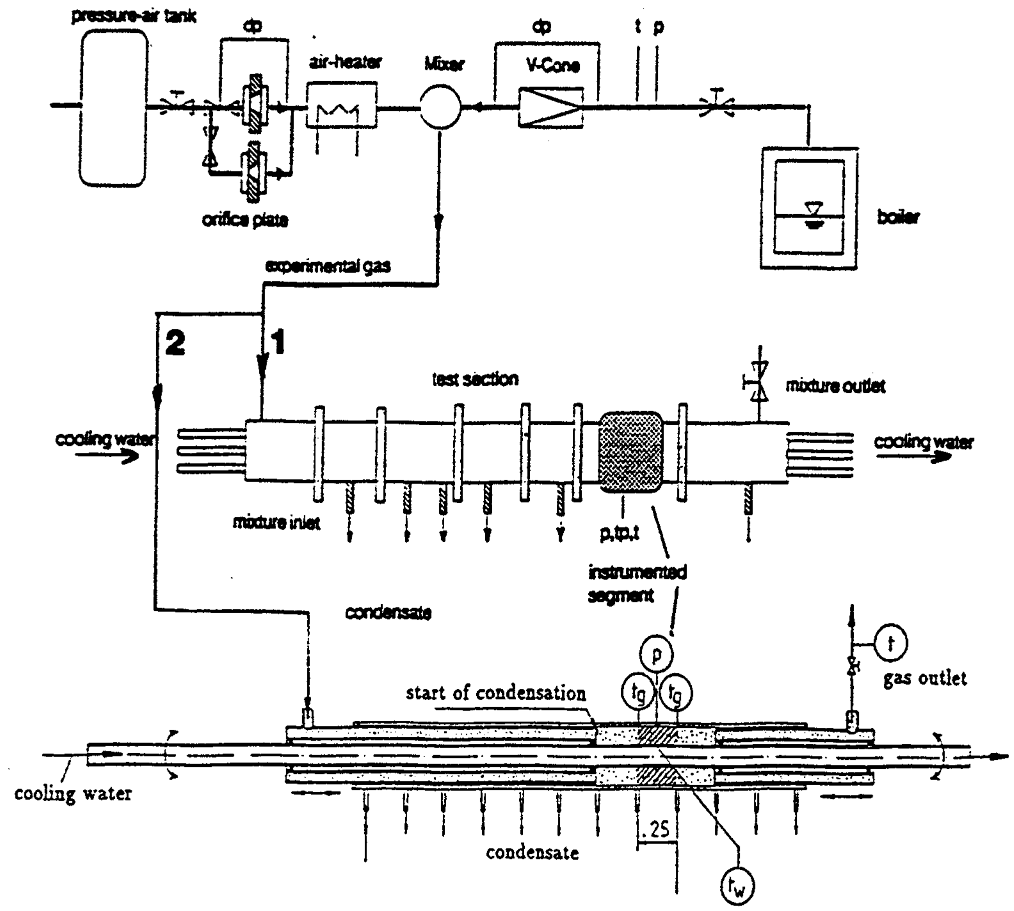

Fig. 1: Schematic of the test loops

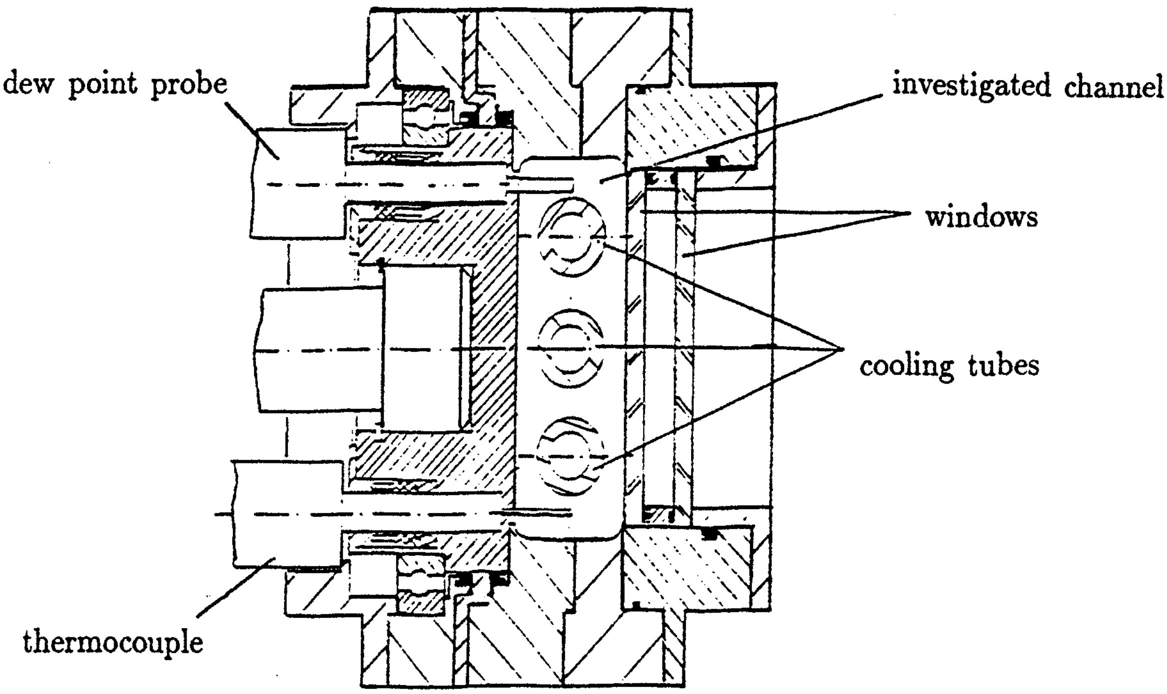

Fig. 3: Cross section of the instrumented segment in the tube row heat exchanger

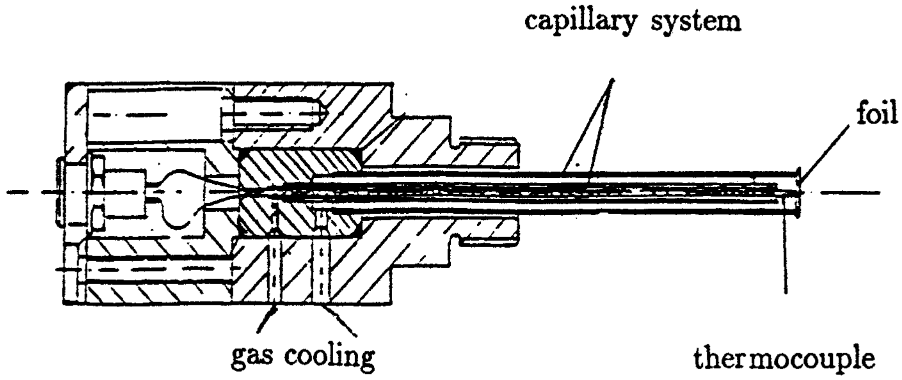

Fig. 4: Dew point probe

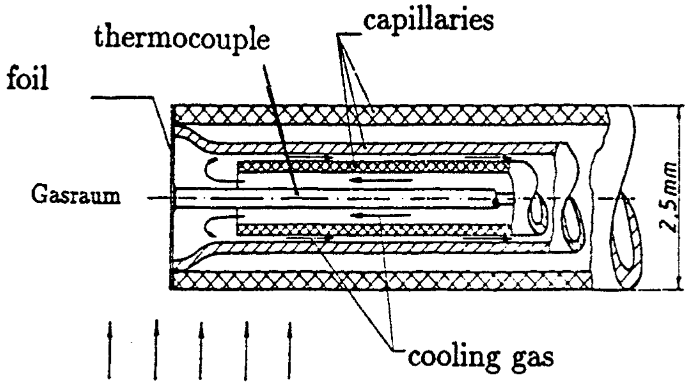

Fig. 5: Top of the dew point probe

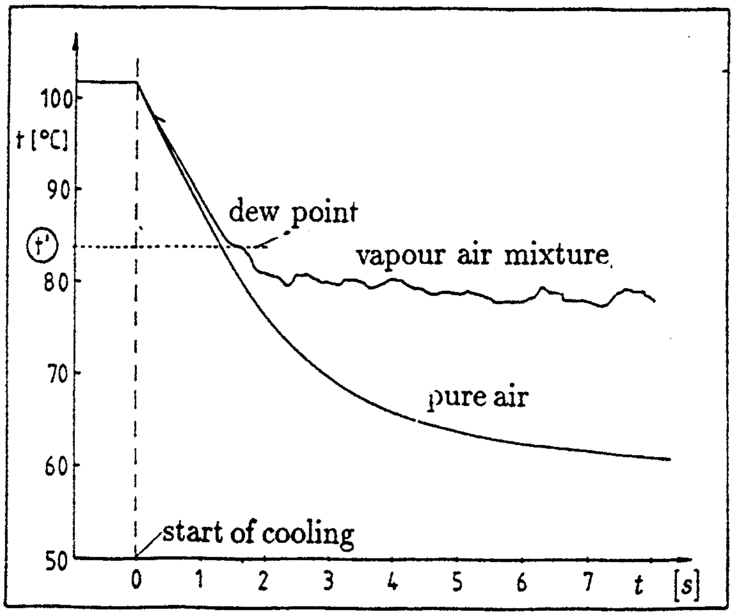

Fig. 6: Temperature curves measured with the dew point probe a) Signal in pure air, b) Signal in a gas air-mixture

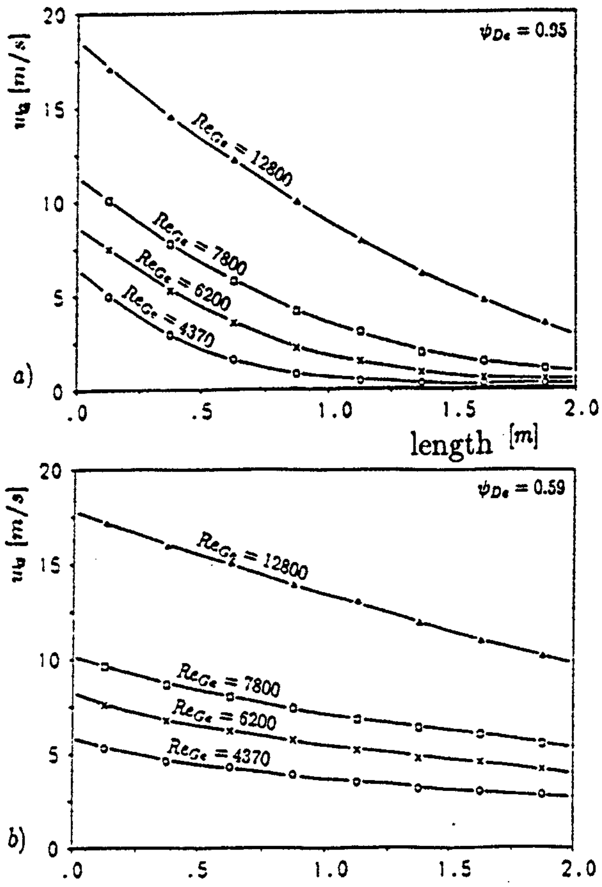

Fig. 7: Velocity in the gas mixture *a*) $\psi_{vi} = 0.95$; *b*) $\psi_{vi} = 0.59$

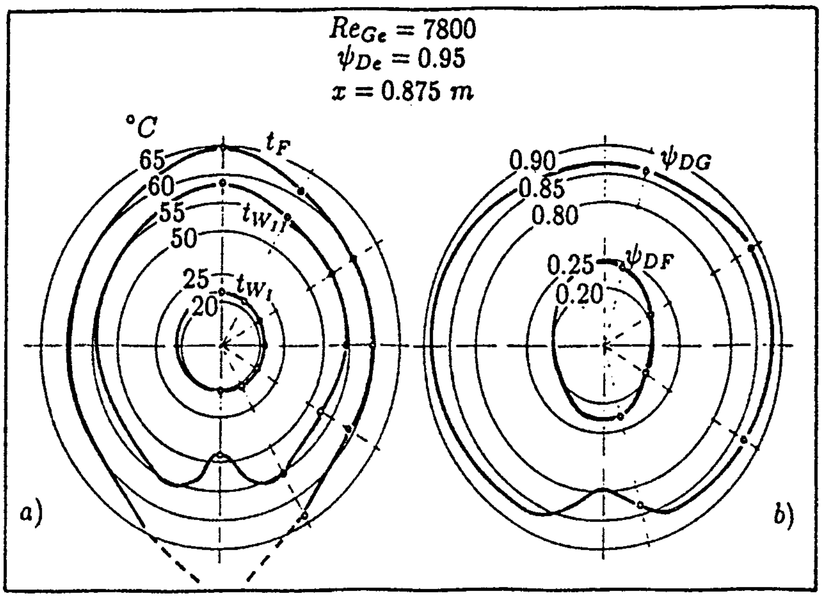

Fig. 8 : Temperature and concentration gradient around the tube a) temperature at the film surface (t_f) and the outer (t_{wII}) and inner (t_{wI}) wall of the cooled tube b) steam concentration at liquid film surface (ψ_{vf}) and outside of boundary layer (ψ_{vf})

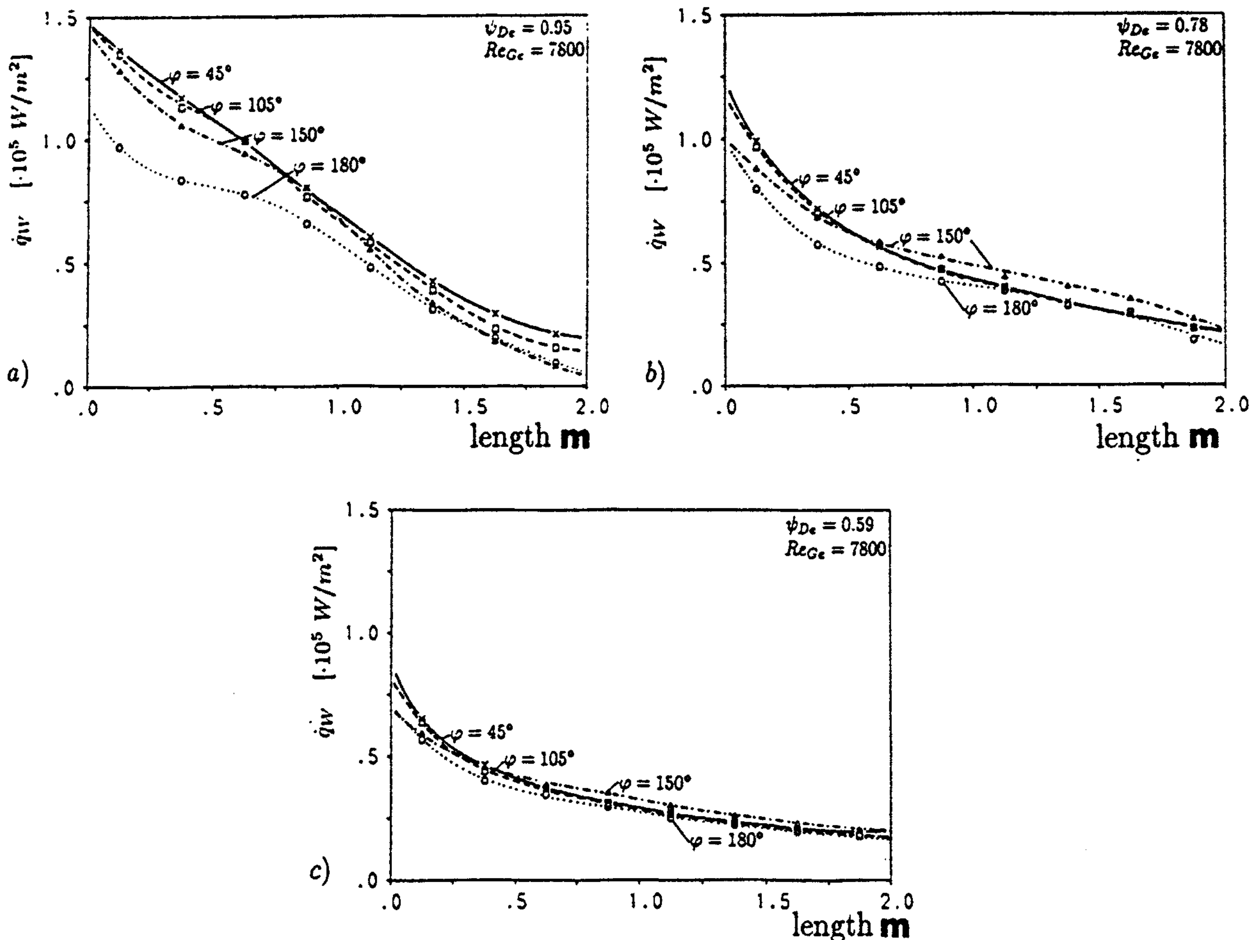

Fig. 9: Heat flux density around the tube (Re_{vi} = 7.800) *a)* psi_{vi} = 0.95, *b)* psi_{vi} = 0.78, *c)* psi_{vi} = 0.59

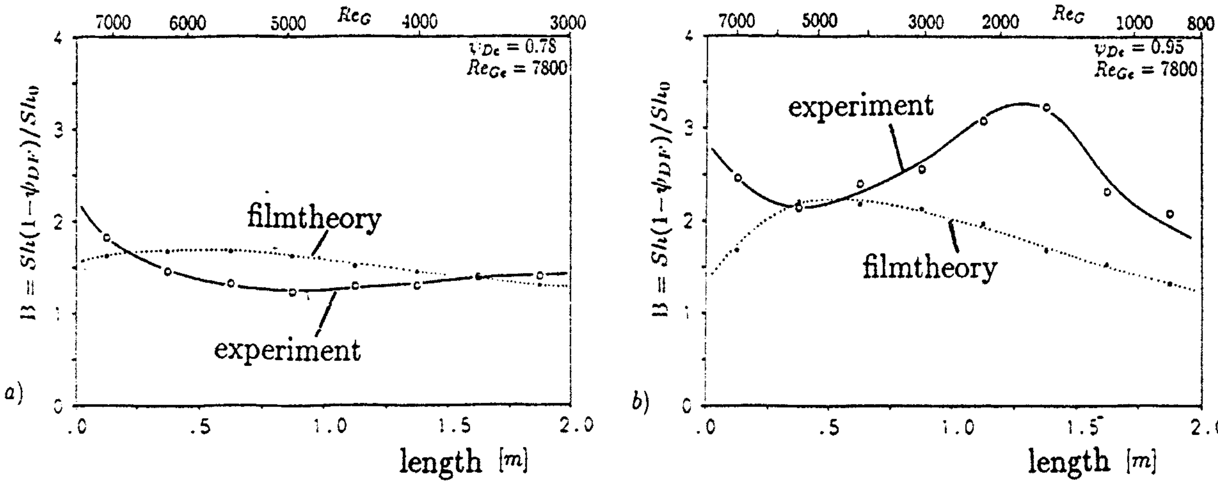

Fig. 10: Correction term B along the cooling tube a) $Re_{mixture} > 3.000$, b) $7.800 > Re_{mixture} > 800$

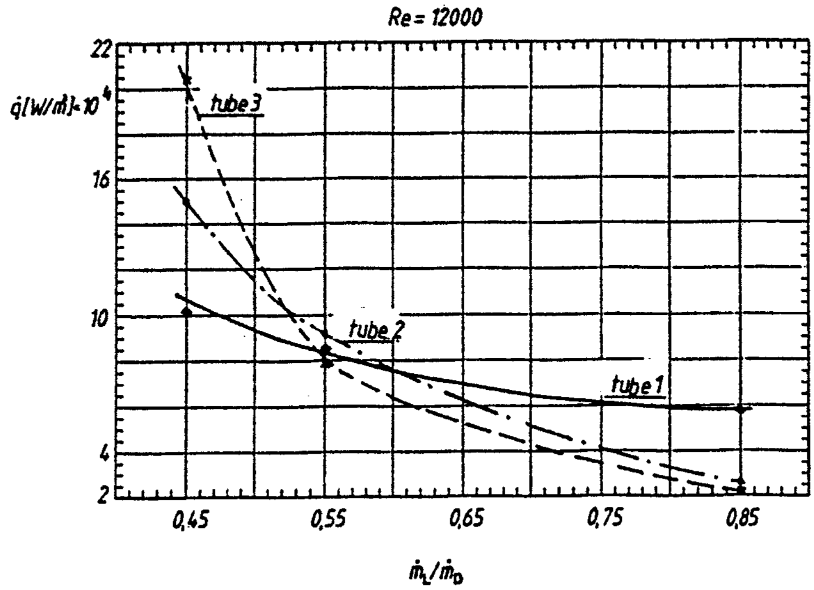

Fig. 11: Heat flux densities after a condenser length of 2m, with constant Reynolds numbers at the inlet

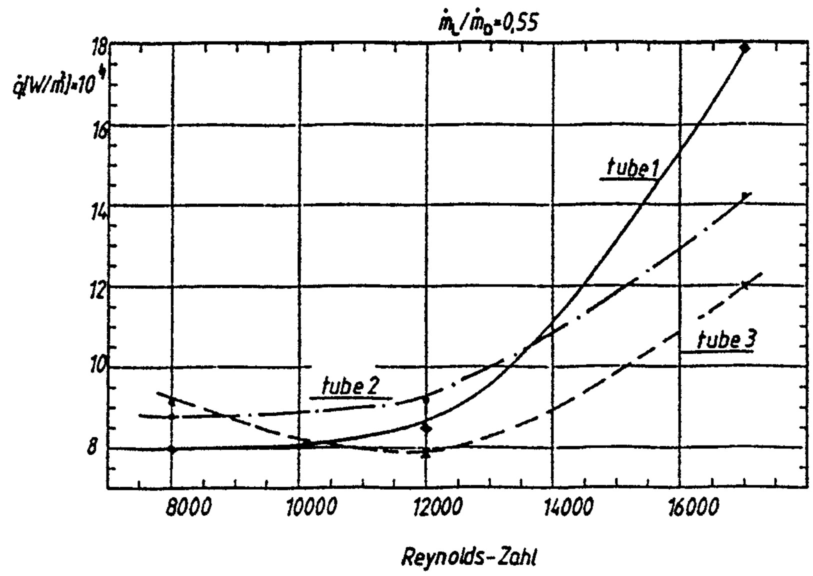

Fig. 12: Heat flux densities after a condenser length of 2m, with constant air/vapour ratio at the inlet